Neural Computing and Applications (2021) 33:14929–14943
https://doi.org/10.1007/s00521-021-06128-x

ORIGINAL ARTICLE

Grid-Tied PV-BES system based on modified bat algorithm-FLC MPPT technique under uniform conditions

Lijun Zhao[1] · Mingxin Jiang[2] · Sajjad Dadfar[3] · Ahmed Ibrahim[4] · Raef Aboelsaud[4] · Farah Jamali[3]

Received: 19 March 2020 / Accepted: 15 May 2021 / Published online: 6 June 2021

Abstract

Grid-connected photovoltaic (PV) systems play an important role in reducing emissions resulting from conventional fossil-fuel-based power plants. However, in order to effectively integrated PV systems into the power system, many challenges regarding these renewable resources such as extracting maximum power under various conditions should be solved. This paper suggests an enhanced maximum power point tracking (MPPT) by the fuzzy logic controller (FLC) and a modified bat algorithm (MBA) to fine-tune the parameters of the controller. The FLC is greatly affected by rule base and membership functions (MFs). The fine-tuning of such parameters cannot be appropriate when accurate information regarding the system is not available. To overcome the above-mentioned challenges, the MBA algorithm is utilized to optimize the scaling factors of MFs. Simulation results confirm that the suggested MBA-FLC method can effectively cope with the global maxima under different weather circumstances with high efficiency, faster tracking and stable output.

Keywords PV · BES · MPPT · FLC controller · Modified bat algorithm

Abbreviations

MBA	Modified bat algorithm
PV	Photovoltaic
MFs	Membership functions
RESs	Renewable energy sources
BES	Battery energy storage
MPP	Maximum power point
AI	Artificial intelligence
HC	Hill climbing
I_{ref}	Short circuit current
K_i	Temperature coefficient
T	Actual temperature
T_{ref}	Reference temperature
G	Solar irradiation (W/m^2)
G_0	Nominal irradiation
V	Open-circuit voltage
R_S	Series resistance
R_P	Parallel resistance
N_S	Number of series cells
X_{best}	Best solution
P_{max}	Upper bound of the power output

✉ Lijun Zhao
zlj99@hebust.edu.cn

1 School of Economics and Management, Hebei University of Science and Technology, Shijiazhuang, Hebei, China

2 Faculty of Electronic and Information Engineering, Huaiyin Institute of Technology, Huai'an, China

3 Department of Electrical Engineering, Saveh Branch, Islamic Azad University, Saveh, Iran

4 Department of Electrical Power and Machines Engineering, Zagazig University, Zagazig, Egypt

1 Introduction

1.1 Motivation and aims

Nowadays, the implementation of sustainable economic development strategies is essential owing to the reduction of fossil-fuel-based resources and environmental problems [1, 2]. Among all types of renewable energy sources (RESs), photovoltaic (PV) power plants have many advantages such as high safety, simple installation, low maintenance cost and environmentally friendly. Therefore, the development of solar power plants is faster than other renewable power plants around the world [3]. Nevertheless, due to the dependence of the output power of solar power plants on solar radiation, their stochastic behavior should be considered [4, 5].

Owing to the stochastic nature of PV systems and also the impossibility of generating electricity during the night, solar power plants must generate power in the distribution networks along with other sources such as storage devices. In other words, due to the impossibility of continuous power generation by PV systems, it is needed for solar systems to operate in combination with battery energy storage (BES) systems [6]. The use of hybrid systems, including solar power plants and BESs, not only solves the problem of the stochastic output of PVs but also it is more cost-effective economically. Nevertheless, it is needed to reduce investment costs to reduce the payback period of hybrid PV-BESs [7]. The use of such a hybrid system provides the capability of storing excess power of PV systems in off-peak periods with low cost to use it in peak times.

1.2 Literature review

For solar power plants, producing the maximum probable power rapidly and reliably in different environmental conditions is significant, which is called MPPT. Accordingly, equipping such renewable resources with a proper MPPT control method is required. In a situation where all the modules of the solar system are illuminated, the power–voltage curve has one single maximum power point (MPP). MPPT controller can greatly increase the efficiency of solar power plants by tracking the peak power point [8]. The first MPPT for PV systems is proposed in 1968 for space applications [9]. Then, various researchers around the world evaluate MPPT controllers based on different indexes such as dynamic behavior, reliable operation, tracking performance, equipment efficiency and simple structure [10]. High speed, low fluctuations at the peak power point and the ability to quickly track output power changes are the main benefits of the proposed optimal MPPT algorithm in the literature. MPPT controllers may be classified on the basis of performance into conventional approaches and advanced (soft computing) techniques [11]. Among various traditional methods, P&O [12], INC, constant voltage and current [13] are common because of simplicity. However, such conventional techniques have the ability to trace the single maximum power point on uniform irradiance [14]. Consequently, traditional MPPT approaches have fluctuations near the global MPP; subsequently voltage perturbations benefit it to properly trace the global MPP [15]. Although traditional MPPT approaches have less complexity than new methods, the use of them in high power applications due to high perturbation rates is not desirable. In other words, the high perturbation rate around the global peak and power oscillations are the main drawbacks of the traditional MPPT control approaches.

On the other hand, tracking performance in new MPPT techniques which are called soft computing, bio-inspired (BI) or artificial intelligence methods (AI) has improved considerably compared to conventional methods [15]. Artificial neural network (ANN) [15], the FLC and heuristic methods are the most popular among different types of improved MPPT techniques. Soft computing-based MPPT plays an important role in finding out the best suitable technique for solving nonlinear problems in the literature due to high-speed convergence and high reliability [16]. Several papers have been published on FLC-based MPPT approaches. These controllers are capable of operating with imprecise inputs; therefore, they do not require precise mathematical modeling and can properly cope with nonlinearity [17]. Nevertheless, the choice of the size of the rule base, the shape and parameters of the membership functions as well as the rule inference mechanism can affect the design of the FLC. In [18], improved MPPT control method based on fuzzy set theory is recommended to enhance the efficiency in a PV system. A fuzzy-based MPPT controller using a small number of rules for a PV system to extract maximum power is suggested in [19]. The proposed method can be easily used for real systems. Another advantage of the fuzzy system is the small memory requirement. However, self-tuning capability is the main disadvantage of the fuzzy-based MPPT controller. To overcome the problem of self-tuning ability, an adaptive FLC for a PV system is recommended in [20]. The proposed method has the ability to change the control parameters under different conditions.

In [21], to overcome the rapid changes of the irradiances in the FLC-based MPPT controller, a particle swarm optimization (PSO) is used for regulating the duty cycle of the DC-DC converter. An improved P&O method is utilized for fine-tuning membership functions (MFs) of the FLC for a grid-tied solar power plant [22]. Even though this scheme provides a high-speed tracking performance, it suffers from oscillations around maximum peak power. In [23], the grey wolf optimizer and random forest algorithms are used at the same time as a novel hybrid MPPT technique. Nonetheless, the major limitation of this scheme is the slow convergence speed. In addition, for rapid variations in irradiances, the initial oscillations at the MPP are very high.

Overcoming the uncertainties in the output power of RESs is another major challenge in the use of hybrid generating technologies. Hybrid PV-BES systems can enhance the reliability and stability of a network supplying with stochastic renewable energy generation [17–21]. In fact, the use of BESs in combination with a solar system can effectively address the problem of the intermittent and stochastic behavior of PV systems. So far, numerous studies have attempted to design proper control methods for the hybrid system [24–26].

2 Contribution

In this present paper, an enhanced control system is utilized in the case of a hybrid PV-BES that is coupled to the power system and the MPPT performance is considered for obtaining MPP at changeable temperature and utilizing an intelligent approach. The suggested MPPT scheme is implemented based on the MBA and FLC regulators. The MBA algorithm is responsible for adjusting the MF scaling factors of the FLC and automatically tunes the MFs of output and inputs. An improved PQ control scheme is also suggested for grid-connected mode.

The remainder of this study is structured as: The PV modeling is presented in Sect. 2. BES modeling is given in Sect. 3. The power flow management scheme is designed in Sect. 4. The FLC and MBA are discussed in Sects. 5 and 6, respectively. Section 7 is represented simulation results. Conclusions are given in Sect. 8.

3 PV model

The main components of PV systems are solar cells with p–n junction. They produce photocurrents when exposed to sunlight and act like diodes in the absence of light radiation. Figure 1 shows the solar cell modeling. Since a single solar cell cannot generate high voltages alone, it is needed to join numerous solar cells in parallel and series to procedure PV modules according to Fig. 2. The amount of output power in PV systems is significantly relevant to the level of irradiation and environment temperature. This type of modeling provides a proper tradeoff between simplicity and precision [24].

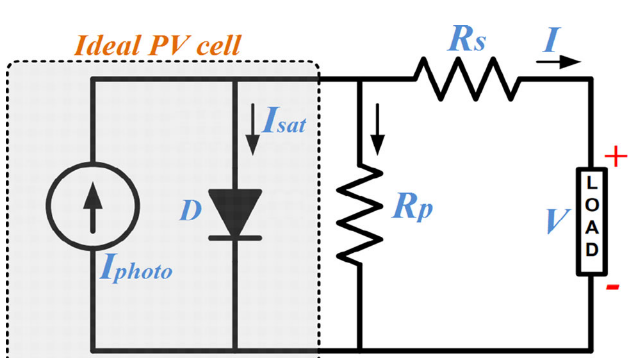

Fig. 1 The solar cell modeling

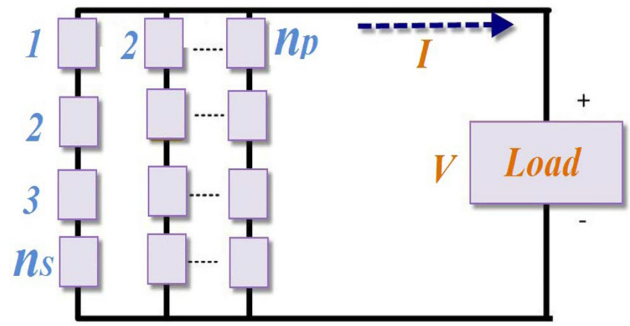

Fig. 2 The model of PV cell, (b) A PV model

$$I = I_{photo} - I_{sat} * \left[\exp\left(\frac{q(V + I * R_S)}{N_S * V_T} - 1\right)\right] - \frac{V + R_S * I}{R_P} \quad (1)$$

$$I_{photo} = \left[I_{ref} + K_i * \Delta T\right] * \frac{G}{G_0} \quad (2)$$

Further details on the modeling of solar systems are given in ref [25–27]. In order to perform the necessary simulations, Red sun 90 W PV module is utilized. PV parameters are represented in Table 1.

Where $I_{MP,}$ V_{MP} and P_{Max} are the current, voltage and power at the maximum power point, correspondingly. N_P stands for parallel cells and N_S indicates the series cells.

4 Battery model

BESs have a significant impact on the economic and sustainable operation of distribution networks, including renewable energy resources [1, 25]. In this article, a lead-acid (LA) battery is used to perform simulations. The use of this type of battery in electrical networks is very common. The BES is joined to the DC bus using a bi-directional DC/DC power converter. In this paper, the power system is used as the backup source to respond to the required demand in conditions of irradiance change or transient periods. In other words, BES can only support the electric network in short-duration times. The major duty of the BES systems is to keep the DC-link voltage at a constant value. Keeping the DC-link voltage constant can provide a stable voltage without any fluctuations, without considering that the battery is charged or not. The

Table 1 Red sun

P_{Max}	V_{OC}	N_S	N_P	I_{SC}	V_{MP}	I_{MP}
90	22.32	36	1	5.24	18.65	4.94

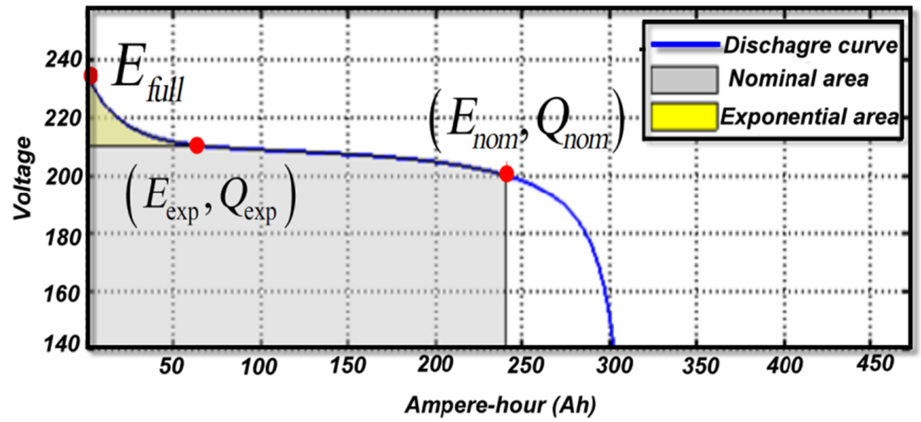

Fig. 3 Discharging characteristics of the battery

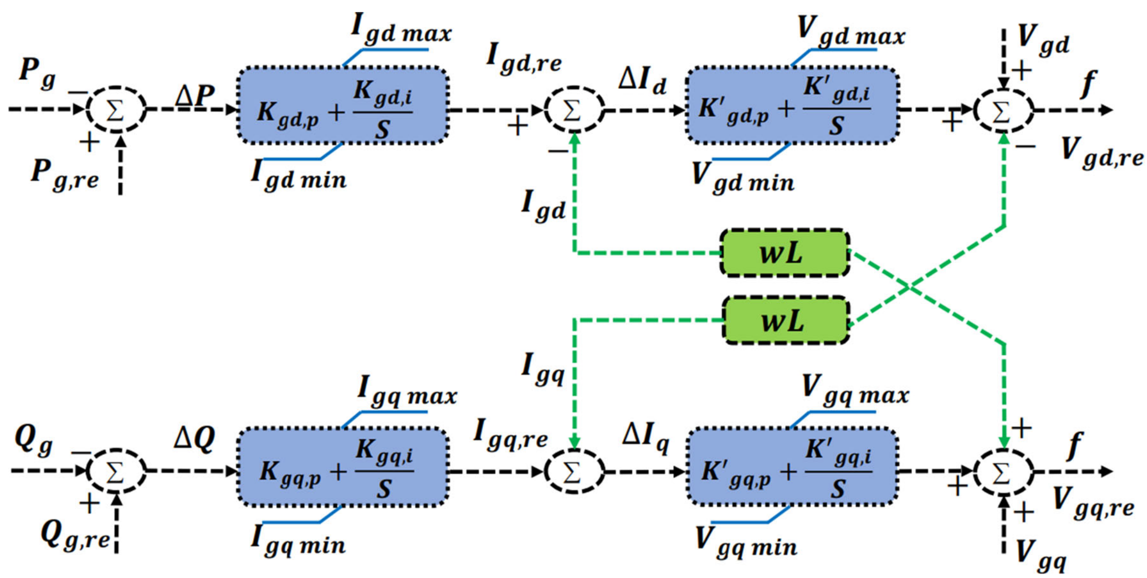

Fig. 4 Conceptual model of the PQ controller

following equation represents the charge/discharge voltage of the battery [17–24]:

$$V_{batt} = E_{batt} - R.I_{batt} \tag{3}$$

E_{batt}, which is the internal battery's voltage, is represented in the following:

Charge: ($i^* < 0$)

$$E_{batt} = E_0 - k_B \frac{C}{i_t + .1C} .i * - K_B \frac{C}{C - i_t} .i_t + \alpha(t) \tag{4}$$

Discharge: ($i^* > 0$)

$$E_{batt} = E_0 - k_B \frac{C}{C - i_t} .i * - K_B \frac{C}{C - i_t} .i_t + \alpha(t) \tag{5}$$

The discharge characteristic of the battery at rated discharging current is shown in Fig. 3. The detailed modeling of the BES is discussed in ref [1].

5 Proposed PQ controller

The most important task of a distributed generation (DG) in grid-tied mode is injecting predetermined power to the network. Injecting the predetermined power of DGs into the distribution networks is done using voltage or current controllers. Here, a current controller is considered for regulating the output power DG units [28, 29]. In the PQ scheme, the output real/reactive powers are used as control parameters and compared with their reference values. The PQ control mode is given in Fig. 4. The output voltage/current (x) can be written as:

$$\begin{bmatrix} x_a \\ x_b \\ x_c \end{bmatrix} = \begin{bmatrix} X_m \cos(wt) \\ X_m \cos(wt - \frac{2\pi}{3}) \\ X_m \cos(wt + \frac{2\pi}{3}) \end{bmatrix} \tag{6}$$

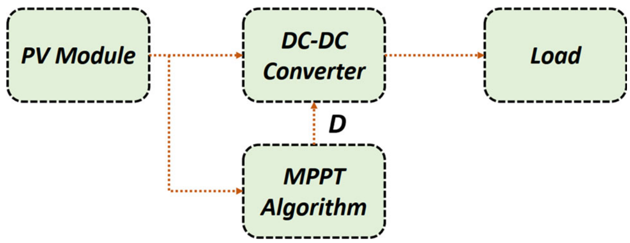

Fig. 5 Block diagram of MPPT method

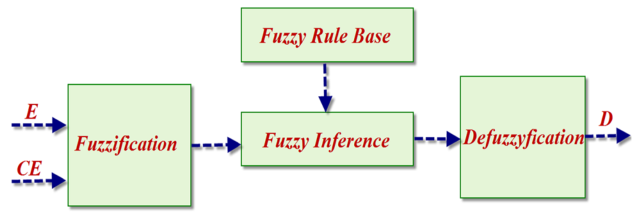

Fig. 6 Block diagram of FLC

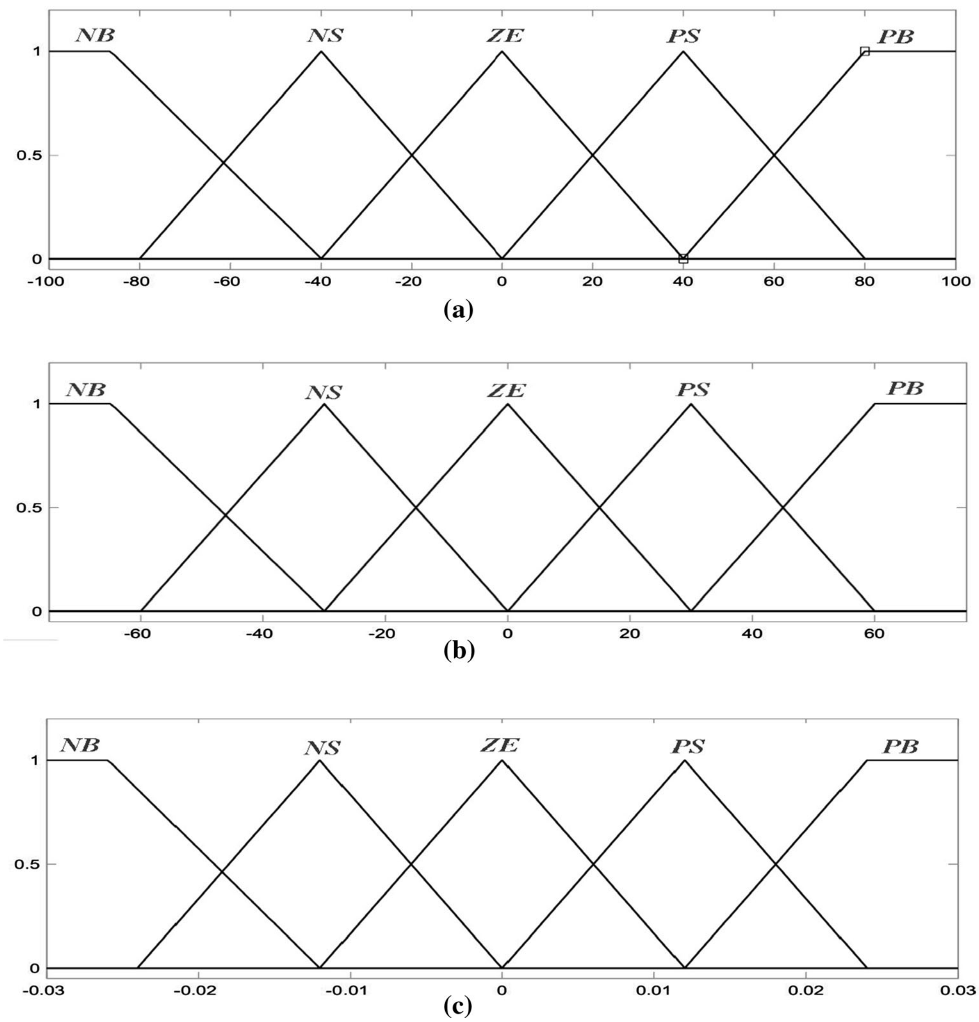

Fig. 7 Membership functions; (a) input; (b) change in input; (c) output

Equation (6) can be represented in the dq frame as:

$$T_{abc\to dq} = \frac{2}{3}\begin{bmatrix} \cos(wt) & cos(wt-\frac{2\pi}{3}) & \cos(wt+\frac{2\pi}{3}) \\ \sin(wt) & \sin(wt-\frac{2\pi}{3}) & \sin(wt+\frac{2\pi}{3}) \\ \frac{1}{2} & \frac{1}{2} & \frac{1}{2} \end{bmatrix} \quad (7)$$

The real and reactive power in the dq frame can also be described as:

$$P = \frac{3}{2}.(v_q i_q + v_d i_d) \quad (8)$$

$$Q = \frac{3}{2}.(v_q i_d - v_d i_q) \quad (9)$$

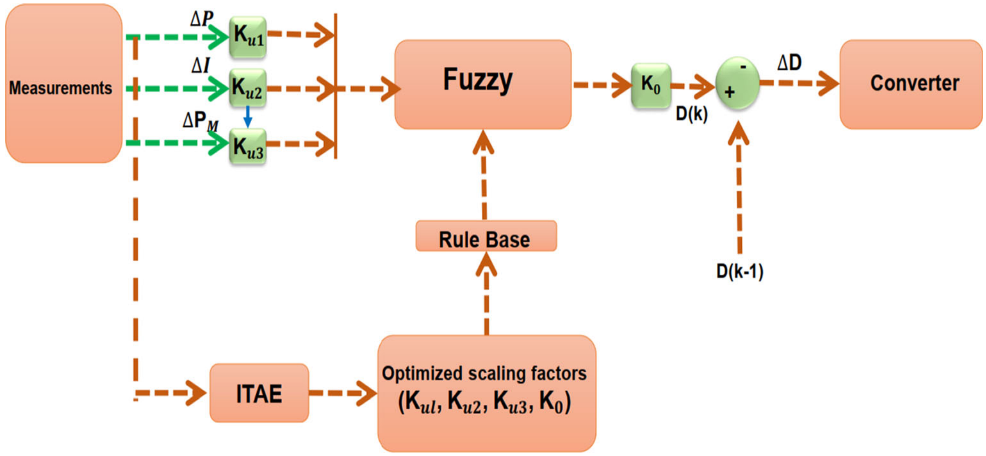

Fig. 8 Proposed Adaptive FLC

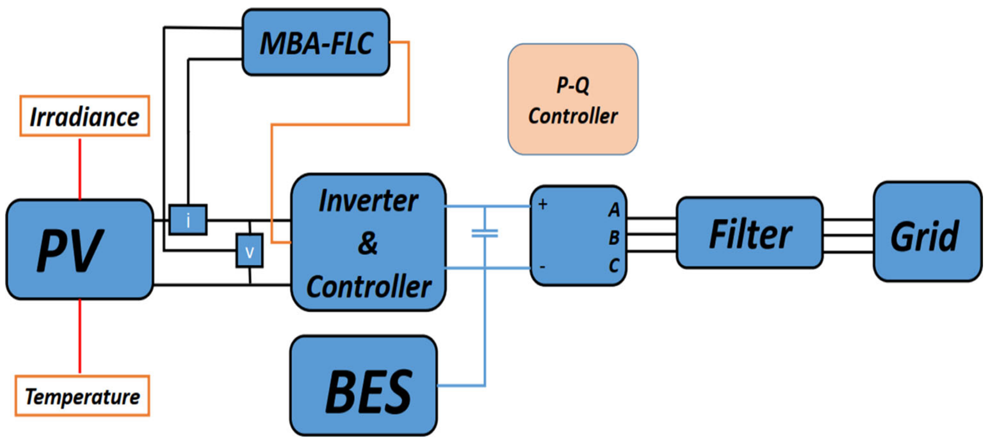

Fig. 9 Proposed control system

Table 2 Parameters of the model

Output power	Load	Carrier frequency	Boost converter
7.3 kW	7.3 kW	5 kHz	L = 3.6 mH C = 625 μF

6 MPPT methods

There are nonlinear characteristics in the solar system such as current–voltage and active power-voltage. These properties can be changed by varying radiation and temperature. Hence, in solar modules, one can change the MMP by changing the ambient conditions. Hence, for producing the maximum power, solar modules were used by a DC-DC converter. In order to obtain the optimal point of operation, the regulator of MPPT is used in PV systems [7]. In the MPPT controller with proper design, there exist important factors that have to be specified between every perturbation (i.e., the maximum step size along with minimum sampling rate). The input-side MPPT regulator is shown in Fig. 5 [8].

6.1 FLC controller

FLC is based on fuzzy set theory which is to some degree similar sets whose components have degrees of membership. The advantages of this method are its simplicity and robustness and no need the precise mathematical model. Moreover, this method has a remarkable ability to deal with the nonlinear behavior of the system, as well as inaccurate inputs and parameters.

FLC mainly contains the four various parts as [6, 24]:

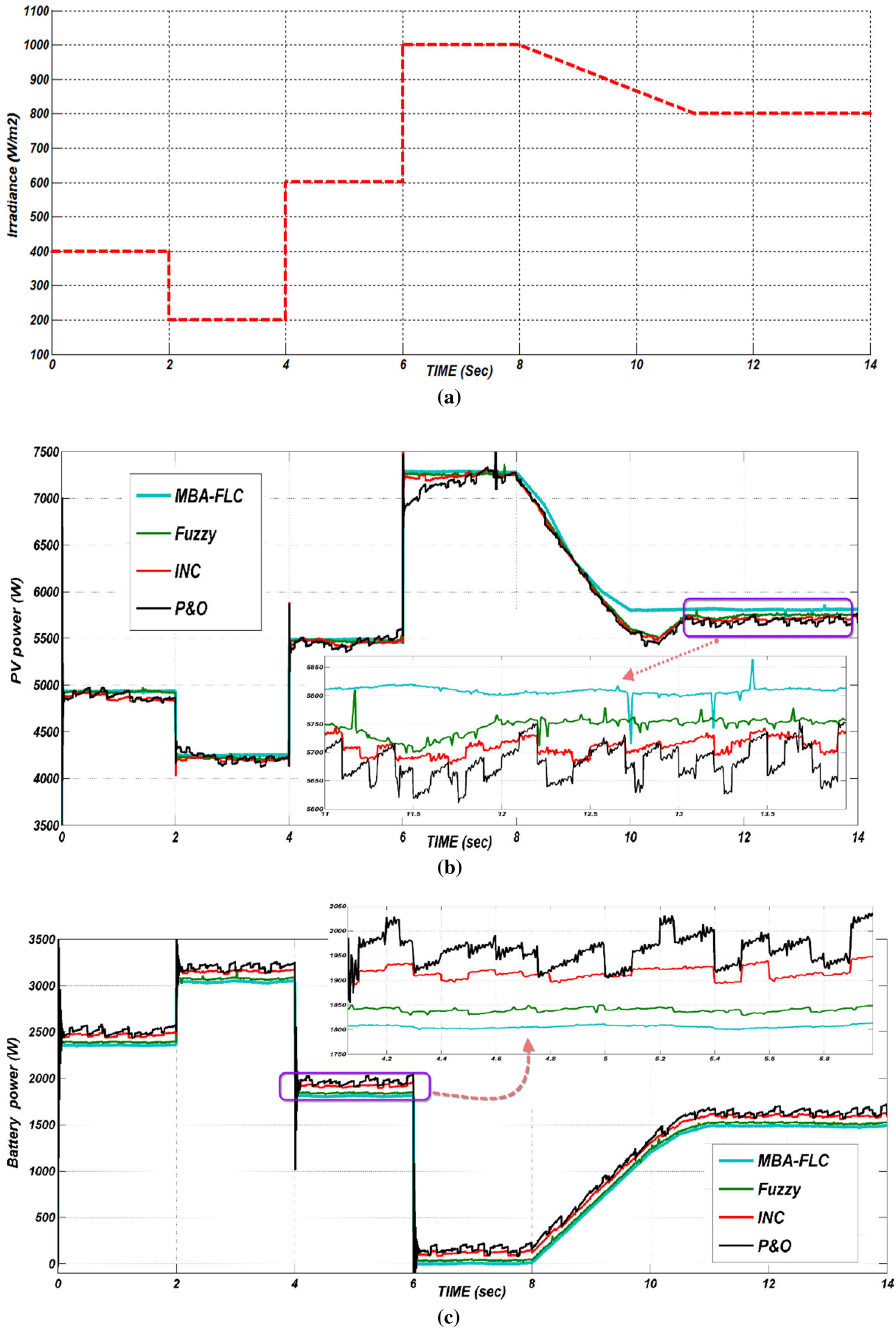

Fig. 10 **a** irradiance variations; **b** PV power; **c** BES power

Table 3 Outputs power of the PV (watt)

Time	Real Value	β Method [34]	HC [9]	P&O [1]	INC [1]	FLC [1]	Adaptive-FLC [1]	MBA-FLC
3–6 S	5056	5016	4998	5003	5031	5040	5041	5047
0–3 S	4364	4332	4318	4325	4345	4350	4353	4358
6–8.5 S	5605	5559	5542	5551	5579	5592	5594	5597
12–14 S	7300	7253	7237	7249	7275	7286	7291	7295
8.5–10.5 S	5926	5879	5864	5871	5898	5908	5918	5921

- Fuzzification: this stage uses for transforming the crisp values into linguistic values.
- Fuzzy inference system: this stage has the capability of expressing logical decisions on the basis of fuzzy concepts and convert the fuzzy rules using the fuzzy concept into the fuzzy linguistic output.
- Rule base: rule base is used to describe the overall control policy of the system.
- Defuzzification: by fuzzy membership functions the fuzzy output values back to actual system values.

The suggested FLC, as presented in Fig. 6, includes two inputs variable and one output variable. Each variable is characterized by seven membership functions as given in ref [6, 24]. E and CE can be calculated as:

$$E(K) = \frac{dP}{dV} = \frac{P_{PV}(K) - P_{PV}(K-1)}{V_{PV}(K) - V_{PV}(K-1)} \tag{10}$$

$$CE(K) = E(K) - E(K-1) \tag{11}$$

E (k) indicates variation in its amount of V-P curve's slope, and ΔD demonstrates variation of duty cycle.

In addition, the variable in output was

$$\Delta D = D(K) - D(K-1) \tag{12}$$

E(k) shows variation for V-P curve's slope,

FLC Toolbox in MATLAB/Simulink is applied for implementing rule base and membership functions. The rule base is presented in Ref [24]. In this paper, the method proposed by Mamdani is used as a fuzzy inference system in which the center method is taken into account for defuzzification. The MFs' output and input variable regarding FLC is depicted in Fig. 7.

6.2 Suggested adaptive FLC based MPPT

In previous FLC control methods, MFs are typically selected incorrectly. However, many authors have recently developed swarm optimization methods to adjust the scaling factors of inputs and output parameters of MFs. Several schemes have been proposed for fuzzy parameter tuning [30]. Here, the MBA algorithm is employed for tuning scaling factors. More details about the MBA algorithm are given in [31]. Figure 8 shows the suggested controller. To decrease the number of variables in the optimization process, the scaling factors of MFs are tuned in preference to fuzzy set ranges. The use of this method leads to reaching the maximum point of power quickly. The integral time absolute error (ITAE) criteria are utilized for the cost function as:

$$ITAE = \int_0^\infty t \times |e(t)| dt \tag{13}$$

6.2.1 MBA

In this part, the MBA algorithm is presented.

6.3 Original BA

The BAT search algorithm operates by imitating the echolocation activities of bats in finding their foods. Yang [31–33] proposes this algorithm to cope with different optimization difficulties. Each virtual bat uses a similar method to update its position. Some of the echolocation characteristics of the bats are used for developing rules related to the BAT algorithm.

a. Bats use echolocation features to differentiate between prey and barrier.
b. Each bat flies accidentally with the velocity at position X_i with a varying frequency fre_i, changing wavelength and loudness to search for prey.
c. Frequency, loudness A_i and pulse released rate of each bat are varied.
d. The loudness varies from a very large amount to a minimum constant amount.

The position and velocity Vel_i of each bat must be introduced and changed. The bat's location is then improved to find the best result [31–33].

The location of each bat is formulated as:

$$\begin{aligned} fre_i &= fre_i^{\min} + \beta\left(fre_i^{\max} - fre_i^{\min}\right) \quad ; i = 1, \ldots, N_p \\ X_i^{new} &= X_i^{old} + Vel_i^{new} \\ Vel^{new} &= Vel_i^{old} + fre_i(X_{best} - X_i) \end{aligned} \tag{14}$$

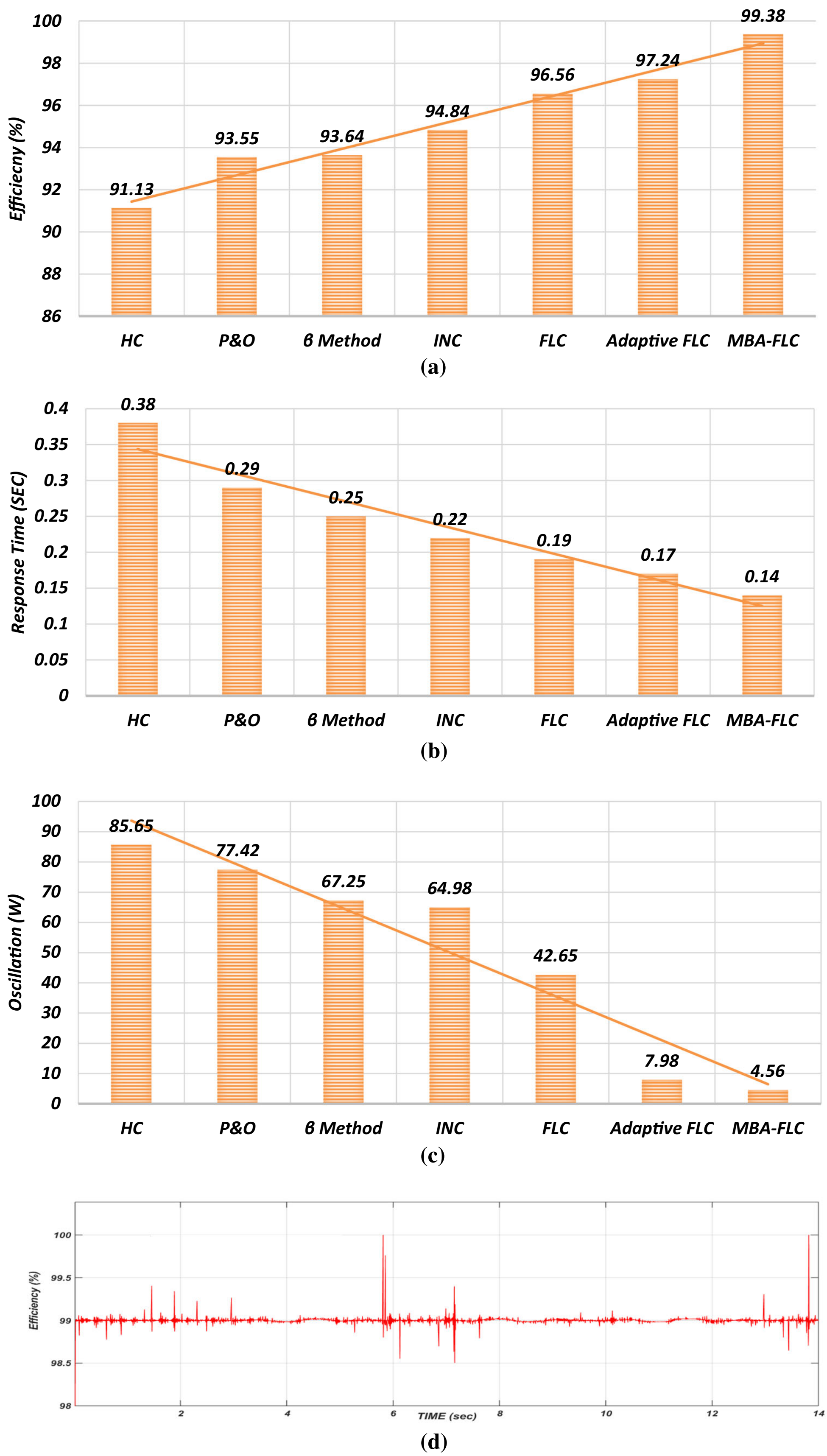

Fig. 11 Irradiance changes: **a** the efficiency; **b** response time; **c** oscillation around MPPT; **d** efficiency of MBA-FLC

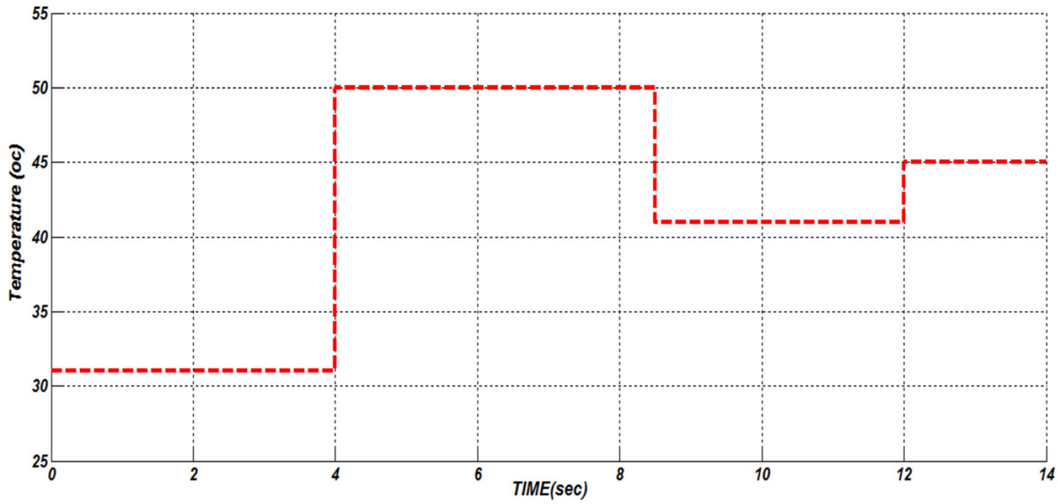
55
50
45
40
35
30
25
Temperature (oc)
0
2
4
6
8
10
12
14
TIME(sec)

(a)

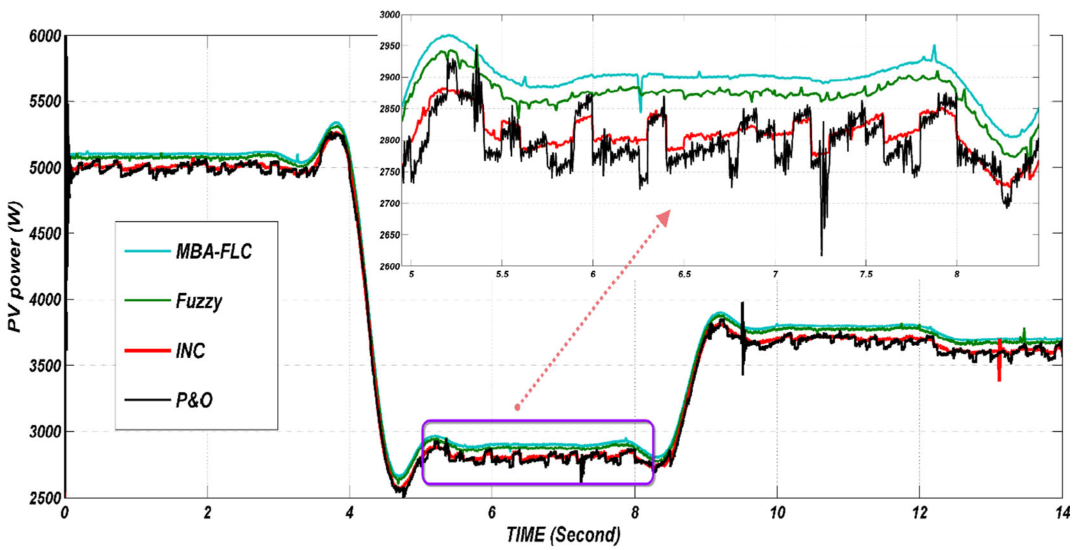
6000
5500
5000
4500
4000
3500
3000
2500
PV power (W)
MBA-FLC
Fuzzy
INC
P&O
0
2
4
6
8
10
12
14
TIME (Second)

(b)

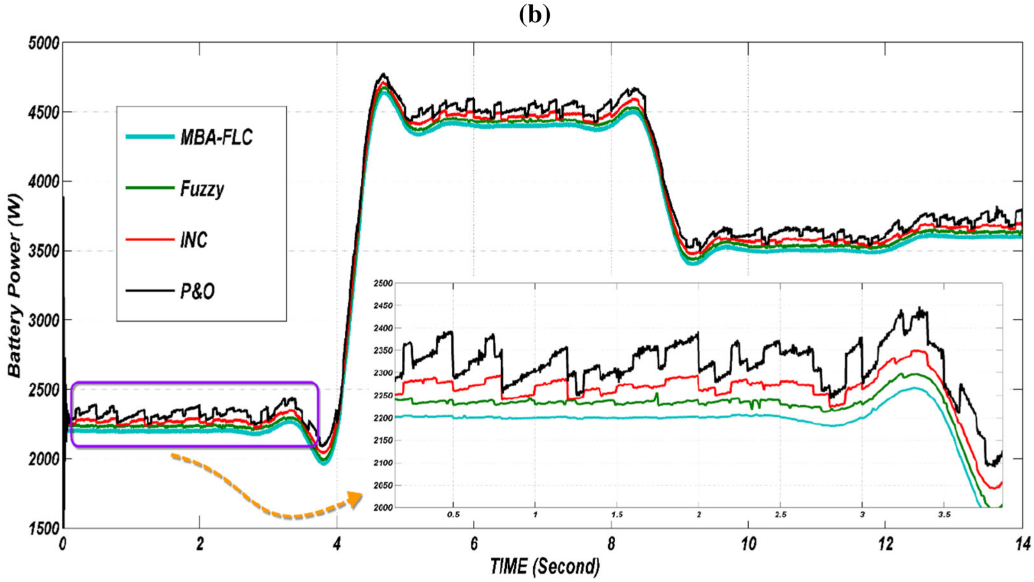
5000
4500
4000
3500
3000
2500
2000
1500
Battery Power (W)
MBA-FLC
Fuzzy
INC
P&O
0
2
4
6
8
10
12
14
TIME (Second)

(c)

◀**Fig. 12** (a) Temperature variations; (b) PV power; (c) BES power

Table 4 Outputs power of the PV (watt)

Time	Real Value	β Method [34]	HC [9]	P&O [1]	INC [1]	FLC [1]	Adaptive-FLC [1]	MBA-FLC
0–4 S	5124	5086	5072	5081	5101	5111	5113	5119
4–8.5 S	2912	2883	2868	2875	2894	2901	2904	2906
8.5–12 S	3874	3841	3827	3834	3853	3862	3864	3867
12–14 S	3725	3687	3674	3681	3702	3712	3714	3717

In order to attain better results, a more updating mechanism has been considered. The second move is a local search around each bat in order to determine the best location in the neighborhood space.

$$X_i^{new} = X_i^{old} + \xi A_{mean}^{old} \;;\quad i = 1, \ldots, N_p \tag{15}$$

A_{mean}^{old} indicates the column-wise mean value of the bat population. If not, a novel possible position X_i^{new} is generated accidentally, ξ is a random number in the range of [-1,1].

$$[\lambda < A_i] \& [f(X_i) < f(X_{best})] \tag{16}$$

λ is the velocity increment.

Then, the rate and loudness of bats is improved as:

$$\begin{aligned} A_i^{Iter+1} &= \alpha A_i^{Iter} \\ r_i^{Iter+1} &= r_i^0 \left[1 - e^{-\rho \times Iter}\right] \end{aligned} \tag{17}$$

where a is a constant in the range of [0, 1].

6.4 Modification method

In this section, three novel modifications are suggested for the BA. The Levy flight is also utilized to make a random walk around each bat. It has a great ability in optimization applications [31–33] and used to enhance the position of each bat X_i as:

$$L\acute{e}vy(\theta) \sim \tau = Iter^{-\theta}; \quad (1 < \theta \le 3) \tag{18}$$

$$X_i^{new} = X_i^{old} + \phi_2 \oplus L\acute{e}vy(\omega) \tag{19}$$

Novel solutions with better position can be replaced with the old bats. Applying the acceleration formulation for enhancing the diversity of the bats population is the second modification. In this process, worse bats move toward the best bats. The acceleration movement of each location X_i to X_{best} is obtained through computing the distance between a bat in the search space and X_{best}. Consequently, the distance of X_i from the best bat in the population X_{best} in each iteration and for each bat X_i is [31, 32]:

$$D = \|X_{best} - X_i\| = \sqrt{\sum_{k=1}^{d} \left(x_{best,k} - x_{i,k}\right)^2} \tag{20}$$

$$X_{best} = \left[x_{best,1}, x_{best,2}, x_{best,3}, \ldots x_{best,d}\right] \tag{21}$$

$$X_i = \left[x_{i,1}, x_{i,2}, \ldots, x_{i,d}\right] \tag{22}$$

where D is the distance of two bats. Then, an attractiveness parameter $\varnothing$ can be described for X_{best}:

$$\phi = \phi_0 \exp(-D) \tag{23}$$

where $\varnothing_0$ is attractiveness of X_{best} with zero distance. Afterward, the position of Xi can be defined as:

$$\begin{aligned} X_i^{new} &= \phi X_i^{old} + (1 - \phi) X_{best} + u_k \\ u_k &= \pi \left(rand - \frac{1}{2} \right) \end{aligned} \tag{24}$$

where π is the absorption coefficient using for controlling the reduction rate. The last amendment technique is implemented on the basis of the crossover operator from the genetic algorithm. For each bat X_i, the crossover operator is provided by the best bat X_{best} as:

$$x_i = \begin{cases} x_{best,k}; \ \varphi_3 \le \varphi_4 \\ x_{i,k} \ ; Else \end{cases} \tag{25}$$

7 Simulation results

In this part, simulations are considered to demonstrate the proper performance of the offered MPPT and power flow control methods. The main objective of the suggested controller is to maximize the output power of PV modules. For simulations, MATLAB/Simulink software is used in two separate case studies.

Figure 9 shows the proposed control scheme. The network operates at 220 V and 60 Hz. Table 2 shows the control parameters. The Red sun 90 W has been employed in the present study.

Fig. 13 Temperature changes: (a) efficiency; (b) response time; (c) variations around MPPT; (d) efficiency of MBAFLC

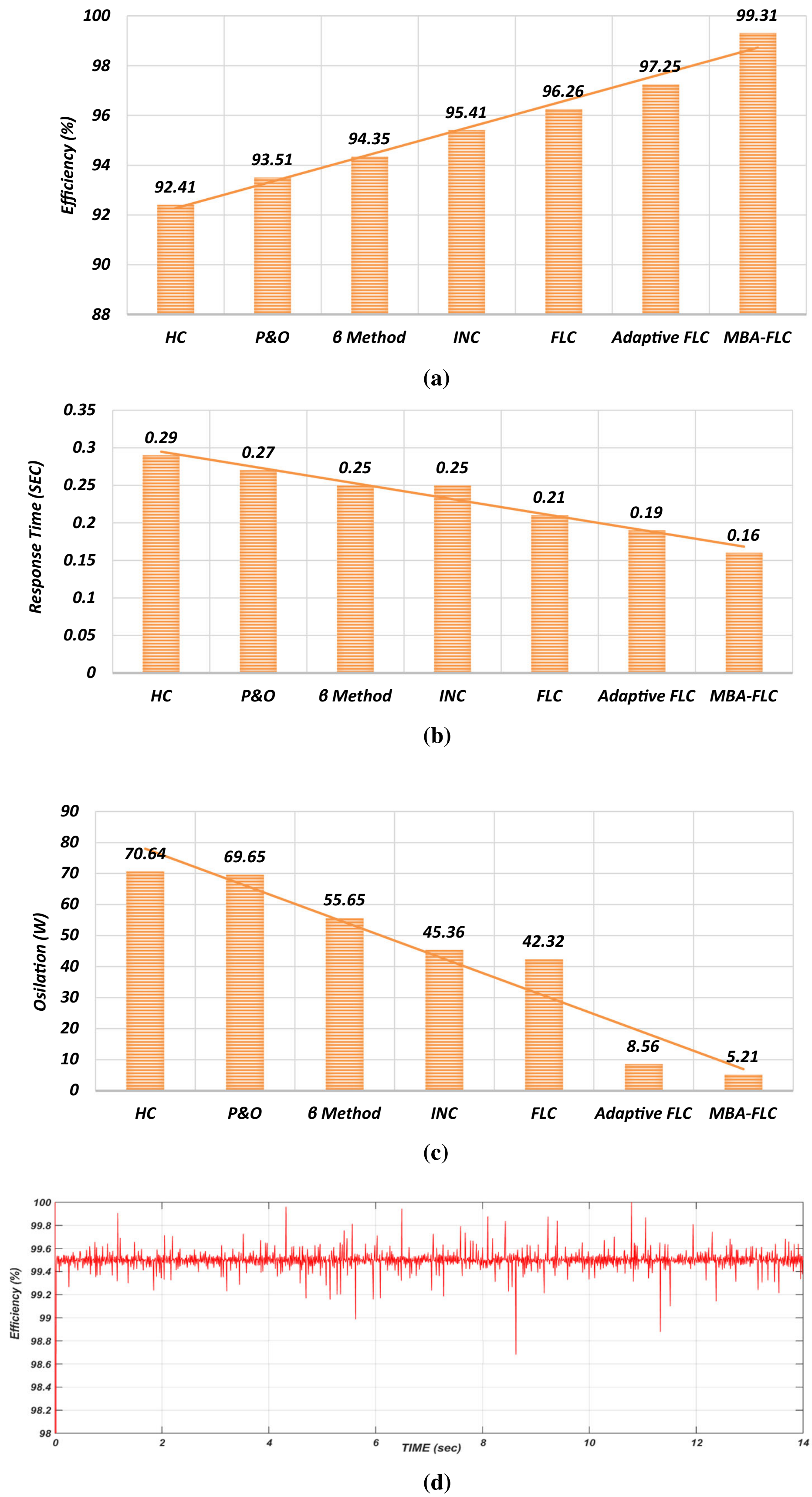

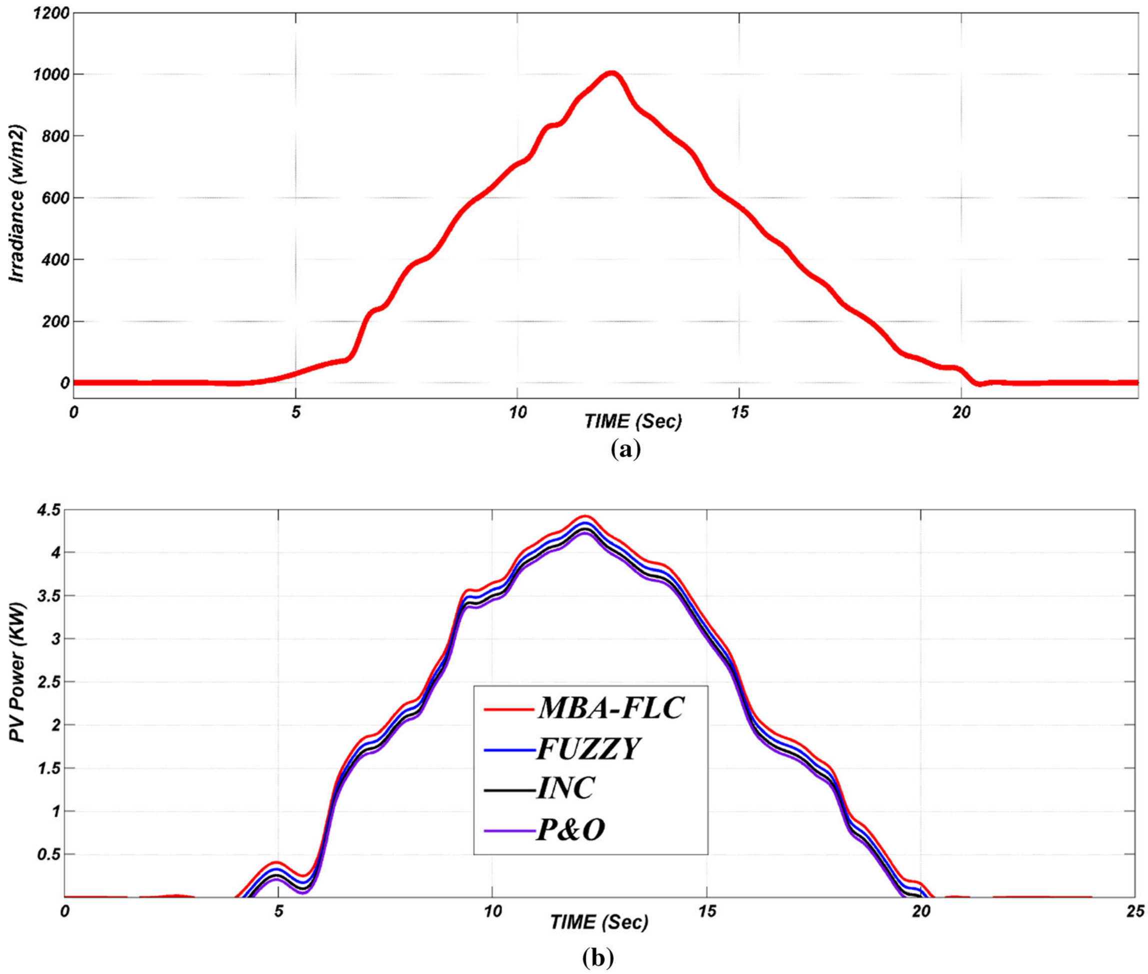

Fig. 14 (a) Irradiance variations. (b) PV system power

The tracking efficiency of the PV system is represented as follows:

$$\eta_{MPPT} = \frac{\int_{t_1}^{t_2} Pdt}{\int_{t_1}^{t_2} P_{\max} dt} \tag{26}$$

7.1 Effect of irradiance

This paper recommends the FLC and the improvement to optimally adjust the MFs of FLC by the MBA to cope with the uncertainties in irradiances. The suggested scheme is investigated in this part, considering that the system functions in the grid-tied circumstances. The solar irradiance is raised in the intervals [0–2 s, 4–6 s] and decreased in the interval [2–4 s and 8–11 s] as shown in Fig. 10a to evaluate the sensitivity of the suggested controller.

The temperature is constant at 25 °C. The behavior of the solar power plant with a quick deviation in solar irradiance is depicted in Fig. 10b. As seen, the suggested control method, i.e., the MBA-FLC, provides a proper performance along with little deviations near the MPP and improved convergence speed. Under various circumstances, the recommended MBA-FLC confirms an improved performance in comparison with conventional approaches. When a sudden change happens in climate situations, oscillations of the operating point are restricted. Considering the irradiance values less than 1 kW/m^2, the output power becomes less than 7.3 kW, and consequently, the utility grid is supplied with active power as shown in Fig. 10c. The achieved values of MPPT related to different values of irradiance are given in Table 3. Moreover, the tracking effectiveness, response time and oscillations around the MPP, considering the variable irradiance are depicted in Fig. 11(a)-(d). Such figures point out that the effectiveness of the proposed scheme is 99%, significantly higher than those attained by other approaches. The suggested MPPT can easily deal with abnormal circumstances.

7.2 Temperature variation

Here, the temperature effect at 1000 W/m^2 is evaluated for the solar system. Considering a rapid change as shown in

Fig. 12(a), the performance of the solar power plant can be attained. Figure 12(b) demonstrates the output power produced by different control approaches, which confirms the improved performance of the proposed method. As seen, oscillations near the MPP happen by means of other approaches when the temperature rises. Additionally, the temperature is reduced at t = 4 s, resulting in a decline in the current. By decreasing the output of the solar system, the utility grid should be supplied the needed power. Figure 12(c) shows the outcomes achieved using various methods for the power delivered by the utility grid, considering the changes in the temperature. Additionally, the results attained for the MPPT by other approaches are given in Table 4. The results for different control methods are shown in Fig. 13 (a)-(c). Besides, Fig. 13(a) demonstrates the efficiency of the MBA-FLC. The attained outcomes confirm that the efficiency of the suggested control method is 99% as given in Fig. 13 (d), significantly higher than other methods. The efficiencies of other methods are all less than 97%.

7.3 Irradiance evaluation in 24 h

It is depicted in Fig. 14(a). Figure 14(b) compares the MBA-FLC with other methods regarding the active power considering different values of irradiance. Figure 14(b) illustrates the associated power output of the PV system with low-speed variations of the solar irradiance and validates the improved performance of the recommended control method. In this regard, an effective theoretical approach is offered for the MPPT to evaluate its behavior in different circumstances.

8 Conclusion

For recyclable nature and eco-friendliness, the PV system is one of the most widely used types of RESs all over the world. However, extracting as much as possible power from the PV systems has been commonly a major challenge in such types of RESs. This paper suggests improved control schemes for a hybrid power system comprising a PV system and battery storage in connection with the main grid. A new MPPT control strategy for the PV system is proposed under various weather circumstances using MBA-FLC. Simulations are provided to confirm the accuracy of the suggested MPPT constraint conditions irrespective of the changing irradiance, temperature or load. The proposed MPPT scheme shows better performance in comparison with conventional control techniques.

Supplementary Information The online version contains supplementary material available at https://doi.org/10.1007/s00521-021-06128-x.

Acknowledgement The study was supported by “Initial Scientific Research Fund of Doctor of Hebei University of science and technology (1181069), China”.

Declarations

Conflict of interest The authors declare no conflict of interest.

References

1. Dadfar S, Wakil K, Khaksar M, Rezvani A, Miveh MR, Gandomkar M (2019) Enhanced control strategies for a hybrid battery/photovoltaic system using FGS-PID in grid-connected mode. Int J Hydrogen Energy 44(29):14642–14660
2. Li Y, Mohammed SQ, Nariman GS, Aljojo N, Rezvani A, Dadfar S (2020) Energy management of microgrid considering renewable energy sources and electric vehicles using the backtracking search optimization algorithm. Journal of Energy Resources Technology. 142(5).
3. Luo L, Abdulkareem SS, Rezvani A, Miveh MR, Samad S, Aljojo N, Pazhoohesh M (2020) Optimal scheduling of a renewable based microgrid considering photovoltaic system and battery energy storage under uncertainty. Journal of Energy Storage 1(28):101306
4. Liu C, Abdulkareem SS, Rezvani A, Samad S, Aljojo N, Foong LK, Nishihara K (2020) Stochastic scheduling of a renewable-based microgrid in the presence of electric vehicles using modified harmony search algorithm with control policies. Sustain Urban Areas 3:102183
5. Hosseini SM, Rezvani A (2020) Modeling and simulation to optimize direct power control of DFIG in variable-speed pumped-storage power plant using teaching–learning-based optimization technique. SOFT COMPUTING.
6. Khan MJ, Mathew L (2019) Fuzzy logic controller-based MPPT for hybrid photo-voltaic/wind/fuel cell power system. Neural Comput Appl 31(10):6331–6344
7. Oshaba AS, Ali ES, Elazim SA (2017) PI controller design using ABC algorithm for MPPT of PV system supplying DC motor pump load. Neural Comput Appl 28(2):353–364
8. Oshaba AS, Ali ES, Elazim SA (2017) PI controller design for MPPT of photovoltaic system supplying SRM via BAT search algorithm. Neural Comput Appl 28(4):651–667
9. Liu F, Kang Y, Zhang Y, Duan S (2008) Comparison of P&O and hill climbing MPPT methods for grid-connected PV converter. In2008 3rd IEEE Conference on Industrial Electronics and Applications. (pp. 804–807). IEEE.
10. Jana S, Kumar N, Mishra R, Sen D, Saha TK (2020) Development and implementation of modified MPPT algorithm for boost converter-based PV system under input and load deviation. International Transactions on Electrical Energy Systems 30(2):e12190
11. Basha CH, Bansal V, Rani C, Brisilla RM, Odofin S (2020) Development of cuckoo search MPPT algorithm for partially shaded solar pv sepic converter. InSoft Computing for Problem Solving. (pp. 727–736). Springer, Singapore.
12. Kim JC, Huh JH, Ko JS (2020) Optimization Design and Test Bed of Fuzzy Control Rule Base for PV System MPPT in Micro Grid. Sustainability 12(9):3763

13. Messalti S, Harrag A, Loukriz A (2017) A new variable step size neural networks MPPT controller: Review, simulation and hardware implementation. Renew Sustain Energy Rev 1(68):221–233
14. Deniz E (2017) ANN-based MPPT algorithm for solar PMSM drive system fed by direct-connected PV array. Neural Comput Appl 28(10):3061–3072
15. Roy SK, Hussain S, Bazaz MA (2017) Implementation of MPPT technique for solar PV system using ANN. In 2017 Recent Developments in Control, Automation & Power Engineering (RDCAPE). (pp. 338–342). IEEE.
16. Rezvani A, Gandomkar M (2016) Modeling and control of grid connected intelligent hybrid photovoltaic system using new hybrid fuzzy-neural method. Sol Energy 1(127):1–8
17. Elshafei AL, El-Metwally KA, Shaltout AA (2005) A variable-structure adaptive fuzzy-logic stabilizer for single and multi-machine power systems. Control Eng Pract 13(4):413–423
18. Won CY, Kim DH, Kim SC, Kim WS, Kim HS (1994) A new maximum power point tracker of photovoltaic arrays using fuzzy controller. In Proceedings of 1994 Power Electronics Specialist Conference-PESC'94. (Vol. 1, pp. 396–403). IEEE.
19. Simoes MG, Franceschetti NN, Friedhofer M (1998) A fuzzy logic based photovoltaic peak power tracking control. InIEEE International Symposium on Industrial Electronics. Proceedings. ISIE'98 (Cat. No. 98TH8357). (Vol. 1, pp. 300–305). IEEE.
20. Patcharaprakiti N, Premrudeepreechacharn S, Sriuthaisiriwong Y (2005) Maximum power point tracking using adaptive fuzzy logic control for grid-connected photovoltaic system. Renewable Energy 30(11):1771–1788
21. Soufi Y, Bechouat M, Kahla S (2017) Fuzzy-PSO controller design for maximum power point tracking in photovoltaic system. Int J Hydrogen Energy 42(13):8680–8688
22. Al-Majidi SD, Abbod MF, Al-Raweshidy HS (2018) A novel maximum power point tracking technique based on fuzzy logic for photovoltaic systems. Int J Hydrogen Energy 43(31):14158–14171
23. Jain AA, Rabi BJ, Darly SS (2020) Application of QOCGWO-RFA for maximum power point tracking (MPPT) and power flow management of solar PV generation system. International Journal of Hydrogen Energy.
24. Khan MJ, Mathew L (2017) Different kinds of maximum power point tracking control method for photovoltaic systems: a review. Archives of Computational Methods in Engineering 24(4):855–867
25. Nejabatkhah F, Danyali S, Hosseini SH, Sabahi M, Niapour SM (2011) Modeling and control of a new three-input DC–DC boost converter for hybrid PV/FC/battery power system. IEEE Trans Power Electron 27(5):2309–2324
26.] Li J, Danzer MA (2014) Optimal charge control strategies for stationary photovoltaic battery systems. Journal of Power Sources. 258:365–73.
27. Vafaei S, Rezvani A, Gandomkar M, Izadbakhsh M (2015) Enhancement of grid-connected photovoltaic system using ANFIS-GA under different circumstances. Frontiers in Energy 9(3):322–334
28. Blaabjerg F, Teodorescu R, Liserre M (2006) Overview of control and grid synchronization for distributed power generation systems. IEEE Trans Ind Electron 53(5):1398–1409
29. Ge X, Ahmed FW, Rezvani A, Aljojo N, Samad S, Foong LK (2020) Implementation of a novel hybrid BAT-Fuzzy controller based MPPT for grid-connected PV-battery system. Control Eng Pract 1(98):104380
30. Farajdadian S, Hosseini SH (2019) Optimization of fuzzy-based MPPT controller via metaheuristic techniques for stand-alone PV systems. Int J Hydrogen Energy 44(47):25457–25472
31. Bora TC, Coelho LD, Lebensztajn L (2012) Bat-inspired optimization approach for the brushless DC wheel motor problem. IEEE Trans Magn 48(2):947–950
32. Tabatabaee S, Mortazavi SS, Niknam T (2017) Stochastic scheduling of local distribution systems considering high penetration of plug-in electric vehicles and renewable energy sources. Energy 15(121):480–490
33. Bangyal WH, Ahmed J, Rauf HT (2020) A modified bat algorithm with torus walk for solving global optimisation problems. International Journal of Bio-Inspired Computation 15(1):1–3
34. De Brito MA, Galotto L, Sampaio LP, e Melo GD, Canesin CA (2012) Evaluation of the main MPPT techniques for photovoltaic applications. IEEE transactions on industrial electronics. 60(3):1156–67.